



FP7 PROGRAMME

**DORIS - Ground Deformations Risk Scenarios:
an Advanced Assessment Service**

GRANT AGREEMENT No. 242212

COLLABORATIVE PROJECT

START DATE: OCTOBER 1ST 2010

**WP5 - Assessment maps delivery and design of
risk scenarios**

DELIVERABLE No. D 5.4

**Ground-deformation velocity maps and time series by SAR
satellite data**

DOCUMENT INFORMATION

Acronym of lead partner for the deliverable	CNR
Work package	WP 5
Contractual date of delivery	Month 24
Date of delivery	September 2012
Nature	O
Dissemination level	PU

Document Responsible	Paola Reichenbach
Author(s)	Gerardo Herrera Rosa María Mateos María Teresa López Inmaculada García

Release	1
Version	1
Date	10 September 2012

REFERENCE DOCUMENTS

DR-1	Annex I - Description of Work of DORIS – “Ground Deformations Risk Scenarios: an Advanced Assessment Service”
------	---

LIST OF ACRONYMS AND ABBREVIATIONS

ALTAMIRA	Altamira Information
CA	Consortium Agreement
CNR	Consiglio Nazionale delle Ricerche
CP	Civil Protection
DAP	Data Access Portfolio
DInSAR	Differential Synthetic Aperture Radar Interferometry
DOW	Description of Work
DPC	Dipartimento della Protezione Civile
EC	European Commission
ELGI	Magyar Állami Eötvös Loránd Geofizikai Intézet
EO	Earth Observation
ERCS	Emergency Response Core Service
ERS	Emergency Response Service
ESA	European Space Agency
EU	European Union
EUAC	External User Advisory Committee
FOEN	Bundesamt fuer Umwelt
FP	Focal Point
FP7	7th Framework Programme
FTS	Fast Track Service
GAMMA	Gamma Remote Sensing Research and Consulting
GMES	Global Monitoring for Environment and Security
IGME	Instituto Geológico y Minero De España
INSPIRE	Infrastructure for Spatial Information in Europe
IT	Information Technology
NFP	National Focal Point
PGI	Panstwowy Instytut Geologiczny - Panstwowy Instytut Badawczy
R&D	Research and Development
SAFER	Services and Application For Emergency Response
TRE	Tele-Rilevamento Europa
UNIFI	Università degli Studi di Firenze
WP	Work Package



TABLE OF CONTENTS

ABSTRACT	4
1. Description of the SPN technique.....	5
2. The SPN processing of L-band data	5
3. L-Band PS data projection along the steepest slope	8



ABSTRACT

This document describes the comparison methodology and the generated results between processed EO data with available ground truth measurements of deformation and/or additional geo-thematic data in the Mallorca sites proposed in DORIS project.

1. DESCRIPTION OF THE SPN TECHNIQUE

The SPN is an advanced differential interferometric processing technique that incorporates both the PS and SB approaches (Arnaud et al., 2003). The basis of the SPN technique is the separation of the different components of the phase difference: displacement, topographic error, atmospheric effects and the uncertainties in the sensor orbit information. The SPN software uses the DIAPASON interferometric algorithm for handling SAR data, e.g. co-registration and interferogram generation. Linear model fitting methodologies generate 3 main products starting from a set of Single Look Complex (SLC) SAR images: (a) the average displacement velocity along the line of sight (LOS) of every pixel (PS); (b) a map of precise reflector heights (being the difference between the height given by the digital elevation model and the true height of each reflector); and (c) the LOS displacement time series of individual PS. A minimum number of images is required depending upon the wavelength of the SAR sensor, the considered time period, and the temporal lapse among SAR image acquisitions. An increase in the number of images contributes to the improvement of the quantity and the accuracy of the displacement results. The SPN PS approach provides a displacement measurement for the pixels (full resolution) of the study area where the electromagnetic response of the radar signal (backscattering) is stable through time. The SPN SB approach utilises medium resolution interferograms which increase the signal to noise ratio on each pixel but at the expense of reducing the spatial resolution of every pixel (multi-looked resolution). Usually, this approach is applied in rural or vegetated areas where good backscatter points are not so abundant, i.e. landslide areas. In these cases the average interferometric coherence can be used to select the suitable measurement points (PS).

2. THE SPN PROCESSING OF L-BAND DATA

The SPN SB approach was used to process 17 SAR images acquired by ALOS PALSAR satellite (L-band) from January 2007 to May 2010. In order to compensate the topographic component of the interferometric phase we used a 25 m resolution DEM generated by the Geographic Spanish Institute. The generation of 104 interferograms was fixed with a maximum spatial baseline between SAR acquisitions is 3099 m, and 3.4 years the maximum temporal separation. The level of multi-looked applied is 8 x 4, resulting a 37 m x 37 m resolution for every pixel (PS). The SPN processing details are summarized in Table 1.

Table 1: Main characteristics of the SAR datasets, the SPN processing and the results.

Band	L	C	X
Wavelength [cm]	23	5,8	3
Incidence angle	38		
Angle between azimuth and North	13.7		
Orbital track	659 and 660 ascending		
Acquisition mode	Fine beam single/dual polarization		
Resolution in azimuth [m] & range [m]	3.5 x 4.7		
Minimum temporal span between two acquisitions [day]	46		
Max. theoretical velocity [mm/yr]	460		
Temporal span	12/06-03/10		
Number of SAR images	17		
Number of interferograms	102		
Multi-look operation	8 x 4		
Maximum spatial baseline [m]	3099		
Min. mean coherence	0.25		
VLOS			
N°. Detected PS	749709		
$\mu \pm \sigma$ [mm/yr]	- 0.2 \pm 2.27		
[min, max]	[-28.1, 24.5]		
Stability interval [mm/yr]	\pm 2 (71%)		
Vslope			
N°. selected PS	700022		
$\mu \pm \sigma$ [mm/yr]	- 0.5 \pm 2.6		
[min, max]	[-71.3, 24.5]		
Stability interval [mm/yr]	\pm 2 (76% PS)		

The displacement velocity in the Line of Sight (Vlos) is shown in Figure 1. A total amount of 690683 PS were detected in the Tramontana Range (388 PS/km²), measuring an average Vlos of -0.2 ± 2.2 mm/yr in the -28,1 mm/yr to +24 mm/yr range. Taking into account the stability threshold proposed by Colesanti and Wawoski (2006) or Cigna et al. (2012) it is observed that 75% of the PS population is found within the ± 2 mm/yr interval, 15% of the PS show Vlos < -2 mm/yr, and 10% of them a Vlos > 2 mm/yr. Note that positive displacement, towards the satellite, is measured in western oriented slopes where landslides have been mapped (Fig. 1). This apparent uplift movement of the slopes is due to the ascending orbit acquisition geometry of the ALOS PALSAR satellite.

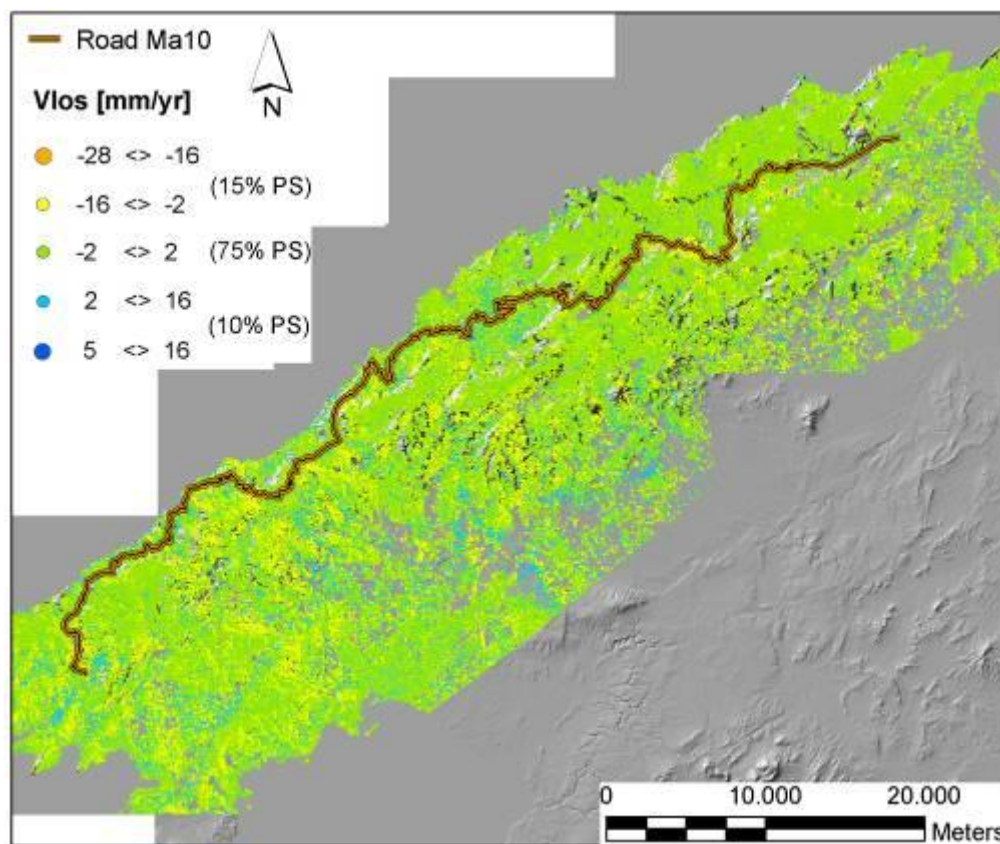


Figure 1. Displacement velocity map (Vlos) obtained from ALOS PALSAR images (06/07-03/10)

In order to eliminate this effect, the Vlos is projected along the line defined by the steepest slope gradient (Vslope) as it is shown in the next section.

3. L-BAND PS DATA PROJECTION ALONG THE STEEPEST SLOPE

The projection of V_{los} along the line defined by the steepest slope gradient (V_{slope}) has been done following the work of Colesanti and Wawoski (2006) and Cascini et al. (2010), using ArcGIS software. As it can be seen in the flow chart (Fig. 2) the V_{slope} value depends on $\cos \beta$ (where β is the angle between the steepest slope direction and the LOS). Therefore V_{slope} tends to infinite when $\cos \beta$ tends to zero (i.e. in layover conditions when β approaches 90°). In order to avoid anomalous solutions a minimum absolute value for $\cos \beta = 0.25$ is fixed for this study area. As a consequence V_{slope} cannot be greater than 4 times the V_{los} (Fig. 2). In the case that V_{slope} turns V_{los} positive, PS is discarded because a positive V_{slope} represents uphill movement. Even though vertical positive displacements may occur at the foot of landslides, the landslide horizontal displacement vector should remain oriented downhill.

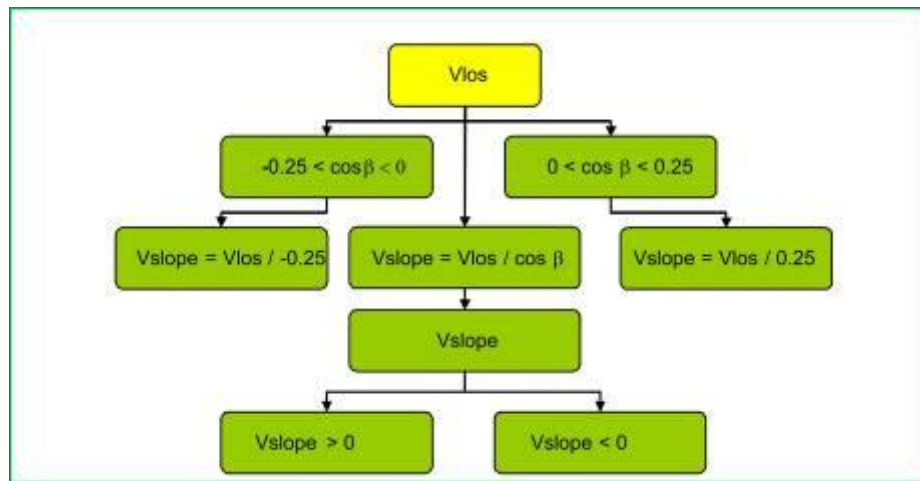


Fig. 2 Flow chart of the V_{los} projection along the steepest slope.

The V_{los} projection along the steepest slope (V_{slope}) are shown in Fig. 3. The PS population was reduced 44% to 389024 PS with a density of 219 PS/km², and an average V_{los} of -3.6 ± 4.5 mm/yr in the $-77,6$ mm/yr to $+22$ mm/yr range. Taking into account the V_{slope} stability threshold proposed by Cigna et al. (2012) it is observed that 73% of the PS population is found within the ± 5 mm/yr interval, 26% of the PS show $V_{los} < -5$ mm/yr, and 1% of them a $V_{los} > 5$ mm/yr.

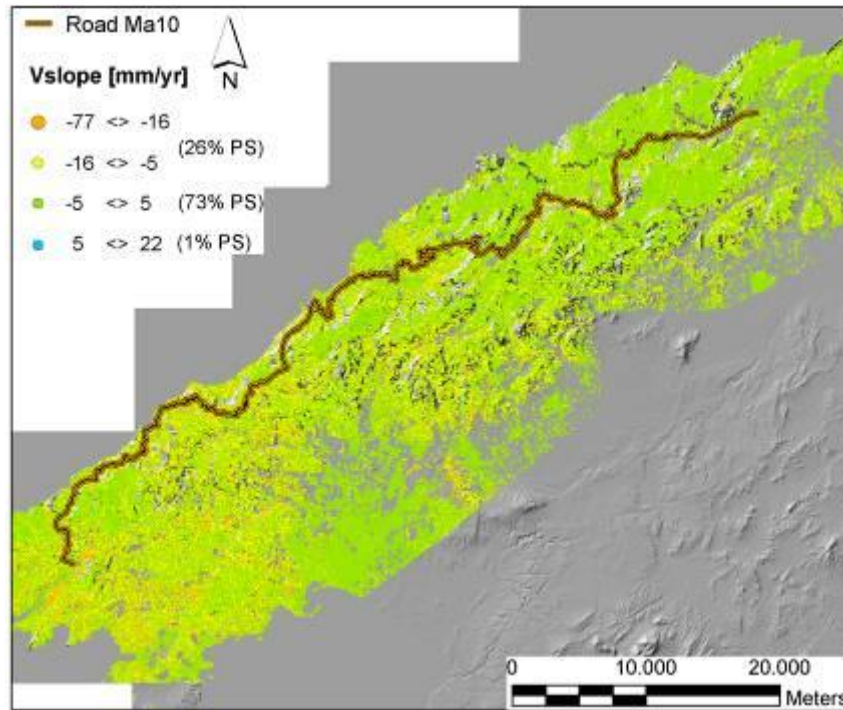


Figure 3. Displacement velocity map (V_{slope}) obtained from ALOS PALSAR images (06/07-03/10)

The observation of Figs. 4a and 4b reveals how useful it is to project V_{los} along the steepest slope in the case that certain slope of interest is oriented to the west. In this case an average V_{los} of $+3 \pm 1$ mm/yr was measured for 21 PS included within the landslide area. This represents an uplift of the whole body of the landslide (towards the satellite) that is due to the acquisition geometry of ALOS PALSAR. Once the V_{los} is projected along the steepest slope an average V_{slope} of -13 ± 4 mm/yr is estimated that is in agreement with the expected landslide displacement to the west.

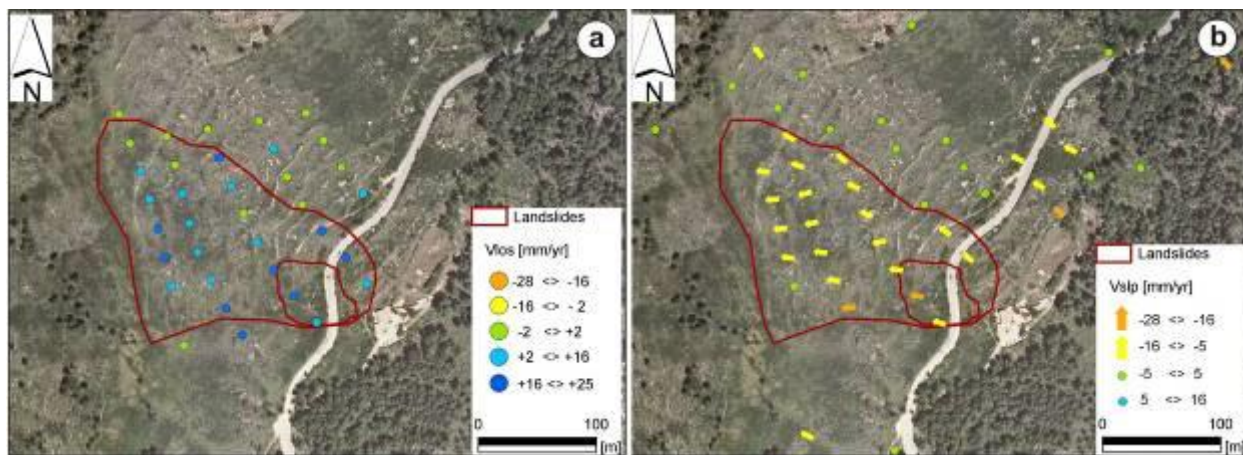


Figure 4. ALOS PALSAR displacement velocity (06/07-03/10) for Estellencs landslide: a) V_{los} ; b) V_{slope}